2024 International Conference on Computer, Electronics, Electrical Engineering & their Applications (IC2E3) | 979-8-3503-8853-4/24/$31.00 ©2024 IEEE | DOI: 10.1109/IC2E362166.2024.10827162

Design and Implementation of Sensor-based Trapezoidal Control of BLDC Motor based on XMC-7200 Microcontroller for EV Application

Chirag Jhawar
Department of Electrical Engineering
National Institute of Technology
Warangal, India
jc22eem1r07@student.nitw.ac.in

Udaya Bhasker Manthati
Department of Electrical Engineering
National Institute of Technology
Warangal, India
ub@nitw.ac.in

Prashant Abhishek
Infineon Technologies.
Bengaluru, India
Abhishek.Prashant@infineon.com

***Abstract*—Nowadays with the exponential growth in technology efficiency is a very critical aspect of any electrical drive system. Using BLDC motors in place of conventional AC induction motors and brushed DC motors can improve efficiency and save energy. In this paper implementation of speed control of brushless DC motor using hall effect sensors with PI controller using XMC 7200 MCU for electric vehicle-type application has been proposed. Block commutation or six-step commutation or trapezoidal control technique is used for the commutation of the phases. This method is straightforward and cost-effective from the implementation of a hardware point of view. A simulation study and hardware implementation have been carried out for this scheme.**

***Index Terms*—BLDC motor, Speed estimation, Block commutation, XMC microcontroller, speed control.**

I. Introduction

The application of BLDC motors is increasing because of the extensive research and growing energy-efficient market of electric vehicles, drones, and many more. Hall sensor-based commutation is often utilized due to its simplicity over sensorless control [1]. The BLDC motor has more advantages compared to the induction machine and brushed DC motor like no friction with brushes, less rotor loss, high efficiency, operate on better power factor, etc. BLDC motor provides high torque and fits in the variable speed application [2]. Despite all these advantages, it has some disadvantages also like hall sensors. These sensors are less reliable and prone to being affected by temperature and vibration. This problem is a hot topic among researchers and many fast fault-tolerant control algorithms are also developed [1]. In the sensored method, the hall sensors are used to get the current position of the rotor, and based on that supply is provided to the appropriate phase to create a rotating magnetic field on the stator. The sensorless control technique eliminates the requirement for hall sensors for commutation. The benefit of the sensorless technique is bypassed by a) the need for a good controller for fast processing of data b) commutation is applied with the help of back emf but back emf is directly dependent on speed-cannot apply this technique at low speed [3]. For this reason, in this paper trapezoidal control method is implemented and discussed [4].

XMC-7200 (stands for cross-market microcontroller) is an industrial microcontroller of Infineon Technologies and is the main control unit. All the commutation, sensing, and processing algorithms are running in the microcontroller. Salient features of this controller are a) 350 Mhz 32-bit Arm cortex M7 CPU and 100 Mhz 32-bit Arm cortex M0+ CPU b) High-performance ADCs of 12-bit with sampling rate up to 1 Msps c) Multiple 32 and 16-bit timers for PWM and counter etc.

FPGA offers a higher degree of flexibility because user can design custom hardware circuits tailored for specific control algorithms but generally requires more time for development because it often involves writing hardware description language (HDL) code and simulating the designs, which can be a lengthy process. XMC microcontrollers are designed with peripherals and features specifically for motor control and power conversion, such as PWM units and ADCs, which can effectively handle BLDC motor control. Development is usually quicker due to the availability of libraries, higher-level programming languages like C/C++, and dedicated development tools like modus toolbox. Typically, for conventional motor control tasks, the preference leans towards XMC microcontrollers due to their straightforward usability, economic efficiency, and targeted range of capabilities. On the other hand, for projects demanding extensively tailored and finely tuned control mechanisms, FPGAs are the go-to choice.

This paper is organized as following sections: In Section II, BLDC motor construction and working is discussed. BLDC motor control scheme is discussed in Section III and Experimental result are shown in Section IV and at the last conclusion in Section V.

II. Construction and working

The construction of the motor is very simple. The stator is the stationary part that has concentrated winding and hall sensors are mounted on the stator. The rotor is the rotating part and is made up of permanent magnets. A voltage source

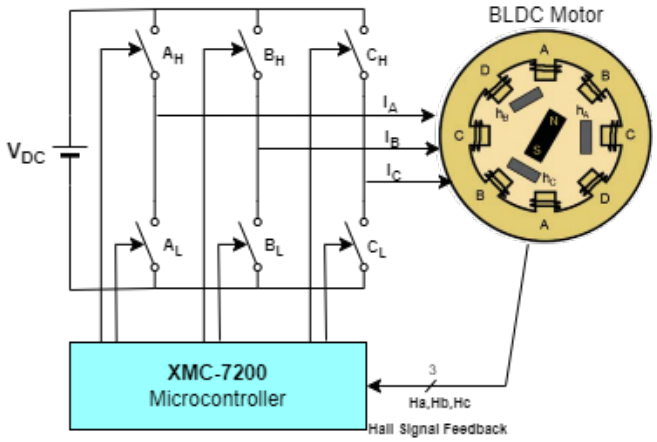

Fig. 1. Block Diagram.

inverter working in 120-degree conduction mode is used to provide a voltage supply to the motor. In this control technique, two phases are in conduction and one phase is always floating. The switches in the same phase have a gap of 60 degrees in conduction so very little chance of a supply short circuit

BLDC motors are electronically commutated motors using hall sensors or encoders. The BLDC motor always works in a close loop. The hall signal fed the position information to the microcontroller. According to the position the microcontroller will generate the PWM pulses to drive the inverter according to the commutation table 1 to generate a rotating electromagnetic field. The close loop diagram of the BLDC motor with microcontroller is shown in Figure 1.

III. Mathematical Modelling

The simplified equivalent diagram of BLDC motor is shown in the figure 2. Voltage equation are shown by (1-3)

$$V_a = V_{an} + V_n = Ri_a + L\frac{d(i_a)}{dt} + E_a + V_n \tag{1}$$

$$V_b = V_{bn} + V_n = Ri_b + L\frac{d(i_b)}{dt} + E_b + V_n \tag{2}$$

$$V_c = V_{cn} + V_n = Ri_c + L\frac{d(i_c)}{dt} + E_c + V_n \tag{3}$$

$$\begin{bmatrix} v_a \\ v_b \\ v_c \end{bmatrix} = \begin{bmatrix} R_s & 0 & 0 \\ 0 & R_s & 0 \\ 0 & 0 & R_s \end{bmatrix} \begin{bmatrix} I_a \\ I_b \\ I_c \end{bmatrix} + \rho \begin{bmatrix} L & 0 & 0 \\ 0 & L & 0 \\ 0 & 0 & L \end{bmatrix} \begin{bmatrix} \frac{dI_a}{dt} \\ \frac{dI_b}{dt} \\ \frac{dI_c}{dt} \end{bmatrix} + \begin{bmatrix} E_a \\ E_b \\ E_c \end{bmatrix} + \begin{bmatrix} v_n \\ v_n \\ v_n \end{bmatrix} \tag{4}$$

$\rho = \frac{d}{dt}$, in the above equation

$$T_e = \frac{E_a I_a + E_b I_b + E_c I_c}{W_m} \tag{5}$$

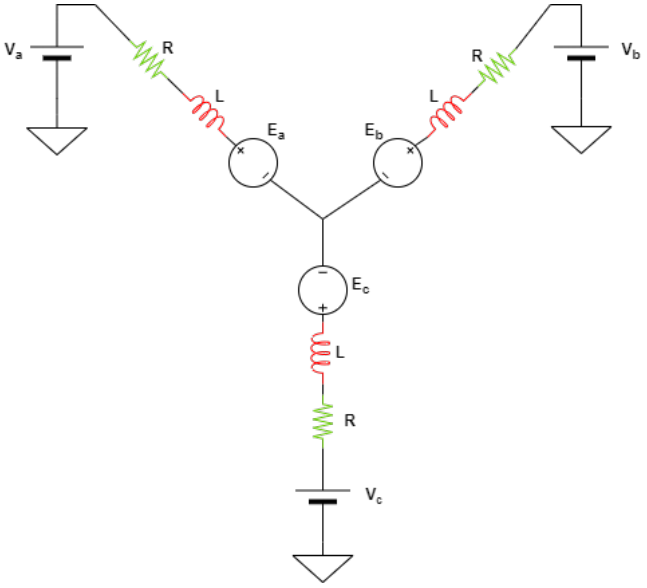

Fig. 2. Simplified Circuit Diagram

$$T_e - T_L = J\frac{d\omega_r}{dt} + B\omega_r \tag{6}$$

$$\omega_e = \frac{P}{2}\omega_m \tag{7}$$

$(\mathrm{V}_a, V_b, V_b - PhaseVoltage)(I_a, I_b, I_c - PhaseCurrents)(E_a, E_b, E_c - PhaseBackEMF)(R_s - PhaseResistance)(L - PhaseInductance)(\omega_e - Electricalspeed)(\omega_m - Mechanicalspeed)$

IV. BLDC motor control

A. Open loop and Commutation Algorithm

Figure 3 shows the flow chart of the commutation and open loop speed control algorithm. The commutation algorithm is necessary to spin the motor. There are three hall sensors on the stator, and it gives the rotor position of the rotor in the form of a digital signal (either 1 or 0) to the microcontroller through 3 pins. The microcontroller decodes the digital signals and converts them to the sectors. The sector information is then passed to the block commutation table. The block commutation table will generate the six combinations of PWM for the inverter switch in each sector. After successfully applying the commutation, the stator will get the supply, and the motor will rotate by 60 degrees. After six commutations the motor will complete one complete rotation. In an open loop speed algorithm, the speed is controlled by an external potentiometer. The speed can vary from zero to full speed.

B. Closed loop

The flow chart for the closed loop algorithm is shown in Figure 5. The algorithm for spinning the motor will remain the same as in an open loop. The right branch shows the implementation of the outer speed loop and inner current loop. The right branch is triggered every 50 microseconds. Control

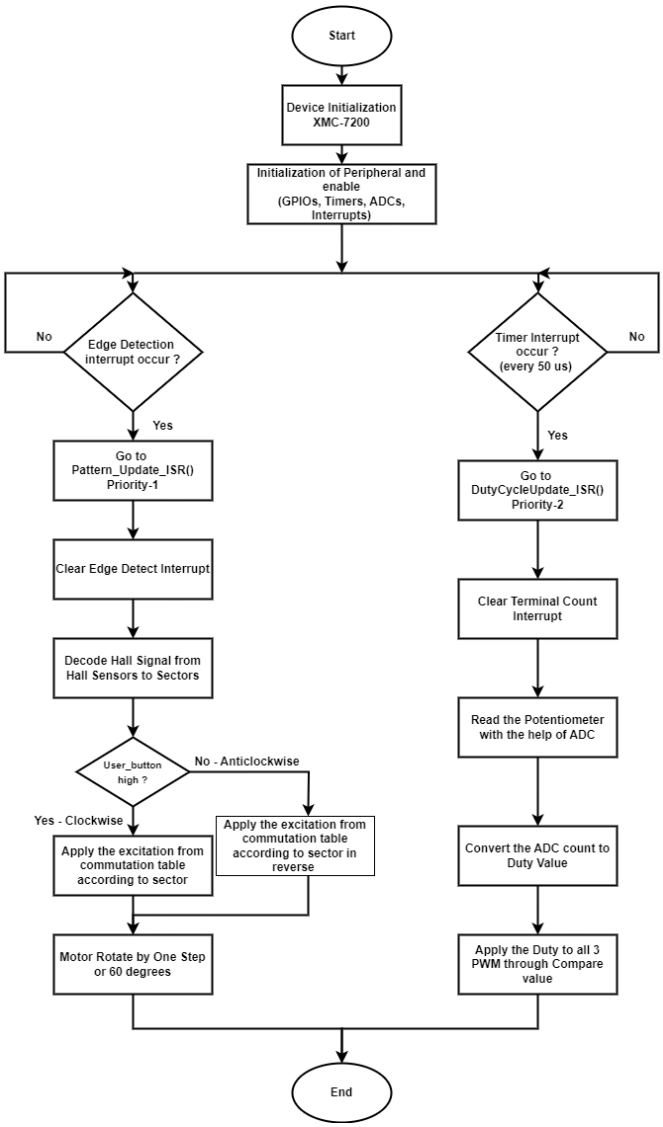

Fig. 3. Flow Chart - Open Loop.

Fig. 4. Commutation table 1.

H1	H2	H3	Sector	A -Phase		B-phase		C-Phase	
				A-H	A-L	B-H	B-L	C-H	C-L
0	0	1	1	0	0	1	0	0	1
0	1	1	3	1	0	0	0	0	1
0	1	0	2	1	0	0	1	0	0
1	1	0	6	0	0	0	1	1	0
1	0	0	4	0	1	0	0	1	0
1	0	1	5	0	1	1	0	0	0
'1' means switch 'ON' and '0' means switch 'OFF'									

is transferred to the ISR, inside the ISR the DC link current sensing and calculation of speed takes place. The calculated speed is fed to the speed PI controller and the output of the controller is a reference current. The sensed DC link current along with the reference current is fed to the current PI controller and the output of the controller is the duty for the PWM signals.

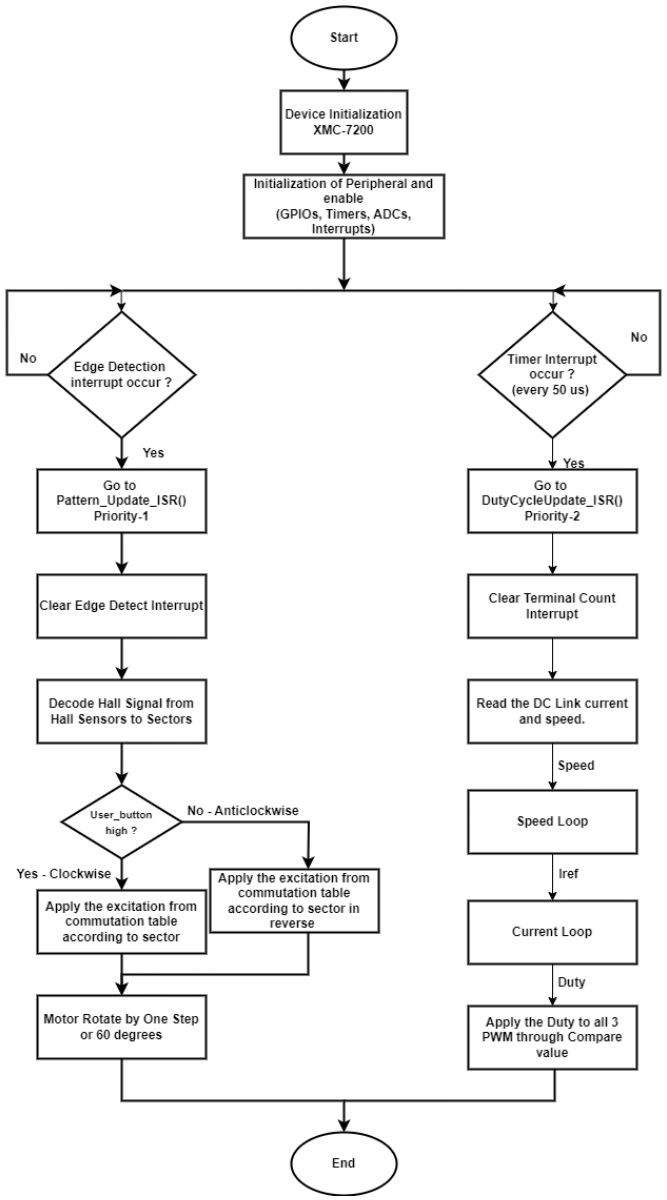

Fig. 5. Flow chart - Closed loop.

The block diagram of the closed-loop system is shown in Figure 6. In a closed loop, the inner current loop and outer speed loop are there. Speed loop provide precise speed control and fast response to changes in speed which is important for electric vehicle applications. The current loop provides improved torque control and enhances protection by limiting the current flowing into the motor. The Back EMF is directly proportional to the motor speed and the torque production is

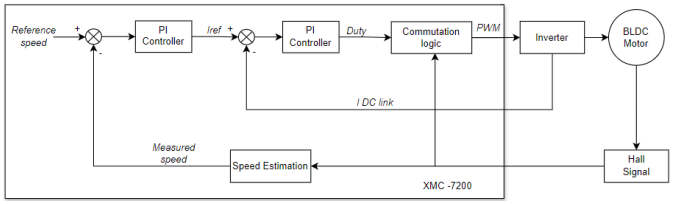

Fig. 6. Closed loop Block Diagram.

almost directly proportional to the phase current.

$$E = 2NlrB\omega \tag{8}$$

$$T = (\frac{1}{2}i^2\frac{dL}{d\theta}) - (\frac{1}{2}B^2\frac{dR}{d\theta}) + (4NBrli) \tag{9}$$

Where N is the number of winding per phase, l is the length of the rotor, r is the internal radius of the rotor, B is the rotor magnet flux density, ω is the motor angular velocity, i is the phase current, L is the phase inductance, θ is the rotor position, R is the phase resistance[4].

The hall signals are changing at every 60-degree interval.The timee between the signal can be noted and the speed can be determined by the equation.

$$\omega = \frac{\triangle\theta}{\triangle t} \tag{10}$$

V. Experimental Results

The hardware used in all experiments is a 3-phase, 24 W, 8-pole BLDC motor. The XMC-7200 Microcontroller evaluation board along with MOT_GPDLV-V2 (general purpose motor drive card) is used for the control unit and voltage supply to the motor. The parameters of the BLDC motor are listed in Table 2. MATLAB/Simulink tool is used to perform simulation. Simulation results are analyzed to prove the feasibility of the system. The experiments are carried out at four conditions a) no load b) full load c) sudden load d) EV load to check the capability of the system. the reference speed varies which depicts the acceleration of an electric vehicle.

Fig. 7. Table-2 Parameters

Specification	Parameters
Number of Phases	3
Number of Poles	4
Voltage Rated (V)	400
Resistance (ohms)	2.98
Inductance (mH)	7
Torque Rated (Nm)	0.7
Rated Speed (RPM)	3000
No load Speed (RPM)	5500
Rotor inertia (Kg-m2)	$0.47X10^{-4}$
Torque Constant (Nm/A)	0.375

A. Results at No load

At no load in figure (8-9), the electrical torque is zero (T = 0). The Motor is operating in an open loop. BLDC motor has the trapezoidal shape of the back emf. For the sake of simplicity back emf waveform of one phase is shown. The back emf waveforms have a 120-degree phase shift. The no-load speed of the motor is 5500 RPM.

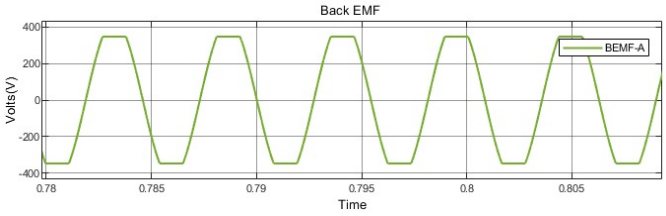

Fig. 8. Trapezoidal back emf waveform at No load.

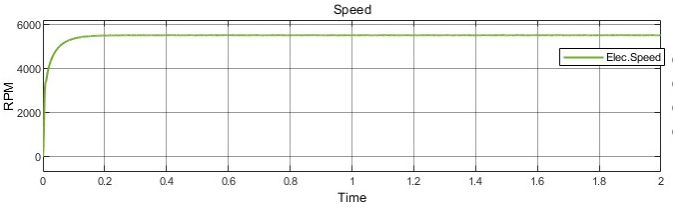

Fig. 9. Speed waveform at No load speed - (5500 RPM.)

B. Results at Full load

All other waveforms remain the same as in no load. The Motor is operating in an open loop. At full load the electromagnetic toque is 0.7 N-m. At full load the Duty of the PWM is 100 %. The speed of the motor is 3000 RPM. The ripple in the motor is because of the block commutation. the waveform are shown in the figure (10-11).

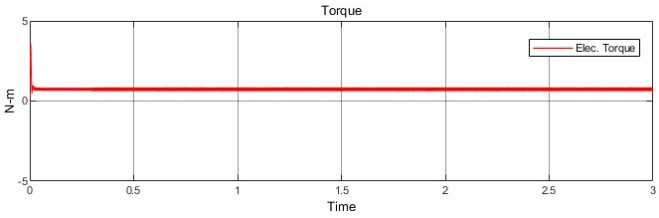

Fig. 10. Torque waveform at full load.

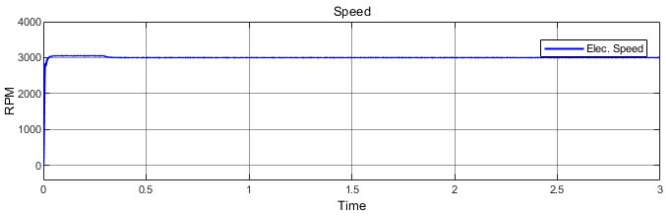

Fig. 11. Speed waveform at full load.

C. Sudden application of load

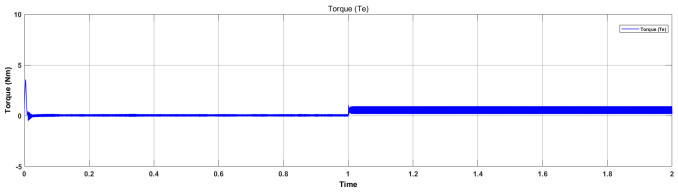

Fig. 12. Torque waveform with applying sudden load.

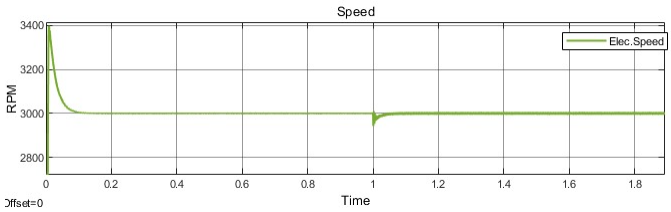

Fig. 13. Speed waveform with applying sudden load.

The Motor is running in a closed loop as shown in figure (12-13). At t=1 sudden load of 0.5 N-m is applied to the motor. The reference speed is 3000 RPM. It can be observed from the Speed graph after the sudden load the speed was reduced but after some time it came back to the reference value because of the closed loop. It took very little time to reach the reference speed again which shows the capability of the system.

D. EV load

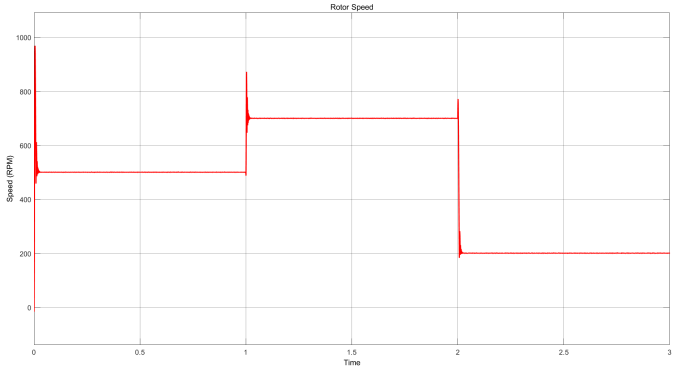

Fig. 14. Speed with EV type of load

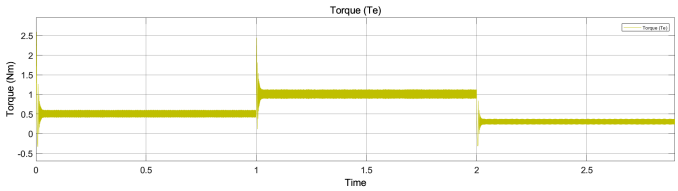

Fig. 15. Torque with EV type of load

Electric vehicles require sophisticated motor control systems to convert electrical energy into motion efficiently. The motor

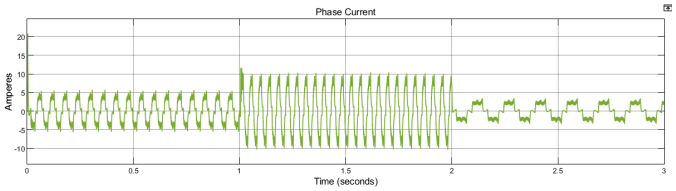

Fig. 16. Current with EV type of load

control system is responsible for controlling the speed, torque, and direction of the electric motor that drives the vehicle. For electric vehicles quick response is important. The acceleration of the electric vehicle is shown in above figure 14-16. Suddenly increase in speed is at t=1 and the sudden decrease in speed is at t=2. In Figure 14 torque is increased, but the speed is not decreasing because of the loops. To fulfill the torque demand the motor is drawing more current from the supply.

E. Hardware results

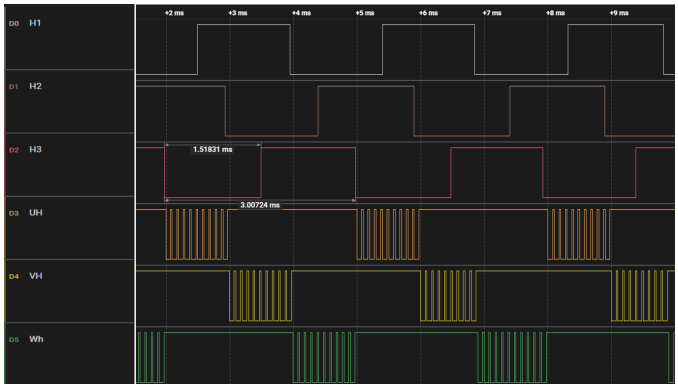

Fig. 17. Hardware PWM and Hall Signals

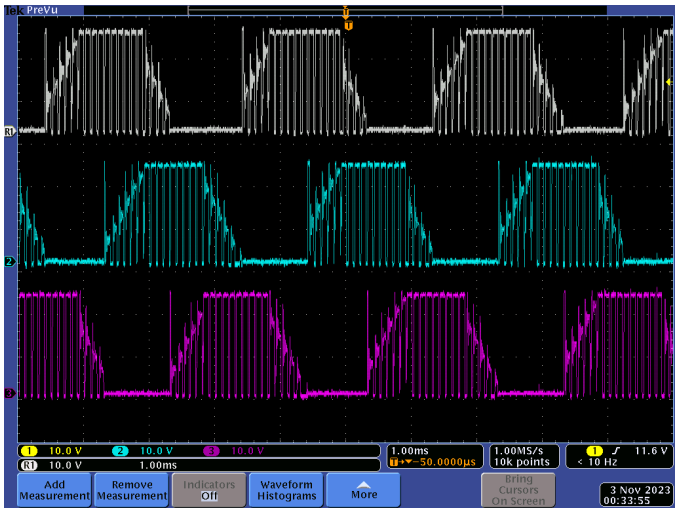

Fig. 18. Practical Back EMF

The experimental waveform of hall sensors and PWM of high-side switches (Modulation) in the inverter is shown in

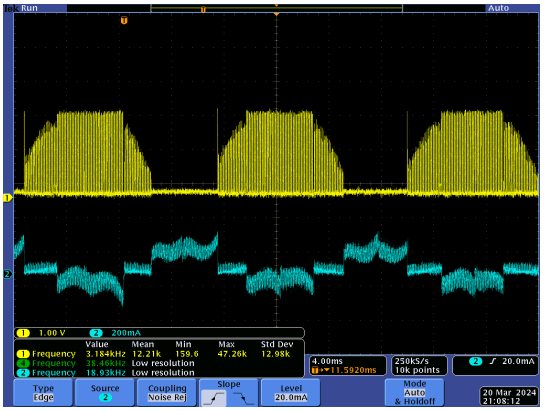

Fig. 19. Current and Back emf waveform

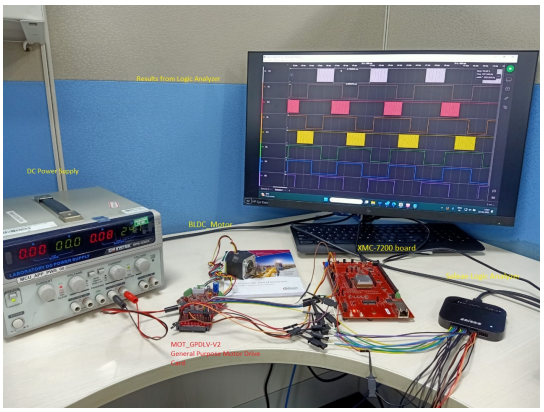

Fig. 20. Experimental setup

Figure 17 The PWM frequency is 20 KHz. The Trapezoidal back emf waveform of all three phases is shown in Figure 18. The waveform of current along with the back emf of phase A is shown in Figure 19. It can be noticed that when the phase is floating the current through that phase is zero. Some spikes in the current waveform are there, it is due to the commutation being applied at that instance.

CONCLUSION

This paper has presented a comprehensive study on the speed control of BLDC motor with hall sensors using XMC 7200 microcontroller. The whole implementation is based on 32-bit XMC-7200 microcontroller. The proposed control algorithm has been shown to effectively control the speed of the BLDC motor in real-time, with high accuracy and stability. The system was able to control the speed of the BLDC motor with high precision and stability, even under varying load conditions. The proposed solution can be used for electric vehicle application. From the results, dynamic response of the system is also very good. The simulation results demonstrate that in close loop motor can run with reference speed.

REFERENCES

[1] M. Ebadpour, N. Amiri and J. Jatskevich, "Fast Fault-Tolerant Control for Improved Dynamic Performance of Hall-Sensor-Controlled Brushless DC Motor Drives," in IEEE Transactions on Power Electronics, vol. 36, no. 12, pp. 14051-14061, Dec. 2021, doi: 10.1109/TPEL.2021.3084921.

[2] H. -C. Wu, M. -Y. Wen and C. -C. Wong, "Speed control of BLDC motors using hall effect sensors based on DSP," 2016 International Conference on System Science and Engineering (ICSSE), Puli, Taiwan, 2016, pp. 1-4, doi: 10.1109/ICSSE.2016.7551633.

[3] "BLDC motor control software using XMC", AP32359, 2017, Infineon Technologies

[4] Bilal Akin C2000, Manish Bhardwaj, Jon Warrine, "Trapezoidal Control of BLDC Motors Using Hall Effect Sensors", SPRABZ4, Texas Instruments.

[5] A. Khergade, S. B. Bodkhe and A. K. Rana, "Closed loop control of axial flux permanent magnet BLDC motor for electric vehicles," 2016 IEEE 6th International Conference on Power Systems (ICPS), New Delhi, India, 2016, pp. 1-6, doi: 10.1109/ICPES.2016.7584148.

[6] P. P. Acarnley and J. F. Watson, "Review of position-sensorless operation of brushless permanent-magnet machines," in IEEE Transactions on Industrial Electronics, vol. 53, no. 2, pp. 352-362, April 2006, doi: 10.1109/TIE.2006.870868.

[7] R. Thapliyal, S. Bose and P. Dwivedi, "An Integrated Bidirectional Multi-Source DC-DC Converter with VMC Approach for VSI-Fed Motor Drive Using Non-Isolated Topology," in IEEE Transactions on Energy Conversion, doi: 10.1109/TEC.2023.3344039.

[8] H. Zhang, L. Deng, H. Li, S. Zheng, H. Jin and B. Chen, "Commutation Point Optimization Method for Sensorless BLdc Motor Control Using Vector Phase Difference of Back EMF and Current," in IEEE/ASME Transactions on Mechatronics, vol. 29, no. 1, pp. 423-433, Feb. 2024, doi: 10.1109/TMECH.2023.3283307.